Research Article
Hittite Journal of Science and Engineering, 2023, 10 (2) 99–116
ISSN NUMBER: 2148–4171
DOI: 10.17350/HJSE19030000297

Novel 1,3,4-Thiadiazole Derivatives as Antibiofilm, Antimicrobial, Efflux Pump Inhibiting Agents and Their ADMET Characterizations

Mahmut Gur[1] Merve Zurnaci[2] Eda Altinoz[3] Nesrin Sener[4] Çigdem Sahin[5] Merve Senturan[3]
Izzet Sener[4] M. Serdar Cavus[4] Ergin Murat Altuner[3]
[1]Kastamonu University, Department of Forest Industrial Engineering, Kastamonu, Türkiye
[2]Kastamonu University, Central Research Laboratory, Kastamonu, Türkiye
[3]Kastamonu University, Institute of Science, Kastamonu, Türkiye
[4]Kastamonu University, Department of Chemistry, Kastamonu, Türkiye
[5]Istanbul Medeniyet University, Department of Engineering Basic Sciences, Istanbul, Türkiye

Article History:
Received: 2022/10/20
Accepted: 2023/05/10
Online: 2023/06/30

***Correspondence to**: Mahmut Gur,*
E-Mail: mahmutgur@kastamonu.edu.tr

This article has been checked for similarity.

ABSTRACT

In this study, 1,3,4-thiadiazole derivatives were obtained from the reaction of benzophenone-4,4'-dicarboxylic acid and N-substitute-thiosemicarbazide compounds with each other. After the synthesis of the final products, some biological properties of these compounds such as antibiofilm, antimicrobial and efflux pump inhibiting efficiencies were evaluated. According to the MBC/MFC test, all the activities were found to be bacteriostatic, also, especially the biofilm inhibition activity of C1 against K. pneumoniae is noteworthy. In addition, C4 was observed to exhibit efflux pump inhibition activity in E. coli, whereas C2 and C3 in K. pneumoniae. The absorption and emission values of the molecules were obtained and electrochemical studies were performed. In addition; absorption, metabolism, distribution, excretion and toxicity (ADMET) scores were predicted using the pharmacokinetic properties of all 1,3,4-thiadiazole compounds. Finally, the electrochemical stabilities of the synthesized molecules have been analyzed by using cyclic voltammetry in 0.1 M TBAPF6 in DMSO as a supporting electrolyte.

Keywords:
Efflux pump inhibition, Antibiofilm, Antibacterial, ADMET, QSAR

INTRODUCTION

When the studies are examined, it has been seen that heterocyclic molecules are generally used for the biological activity tests of the compounds. Thiadiazole rings containing two nitrogens and one sulphur atom are very popular compounds for such studies. In particular, the 1,3,4-thiadiazole isomers are the prominent derivatives in the thiadiazole class in terms of their pharmacological properties. 1,3,4-thiadiazole molecules and their derivatives possess a wide range of pharmacological activities like anticancer/antitumor (1,2), anticonvulsant (3,4), antidiabetic (5,6), anti-inflammatory (7,8), antidepressant (9), antihypertensive (10), antiviral (11,12), antileishmanial (13,14), antimicrobial (15,16) and many more. Among these studies, the most common pharmacological feature is antimicrobial studies. Because of the over/misuse of antibiotics, antibiotic resistance caused by microorganisms is now recognized as a serious global threat. As a precaution against this situation, studies are being carried out for developing novel agents that target the mechanisms of virulence. These studies aim indeed at imposing limited selective pressure on the improving of the antibiotic-resistance (17–19). The ability to form biofilms is one of the major natural resistance mechanisms improved by pathogens and this is the main reason why many infections are difficult to treat with conventional antibiotics (20,21). In recent years, some studies have been done on the synthesis of new molecules that can interfere with biofilm formation suitable for the treatment of biofilm-associated infections (22,23). Generally, inhibitors of biofilm formation are types of compounds that can inhibit microbial attachment to surfaces by interfering with bacterial adhesion. Although there are many studies on 1,3,4-thiadiazole derivatives (24), detailed studies on their biofilm forming properties are scarce.

Based on all these situations described in detail, we synthesized 1,3,4-thiadiazole derivatives, from

Cite as:
Gur M, Zurnaci M, Altinoz E. & et al. Novel 1,3,4-Thiadiazole derivatives as antibiofilm, antimicrobial, efflux pump Inhibiting agents and their ADMET characterizations. Hittite J Sci Eng. 2023; 10(2): 99-116. doi:10.17350/hjse19030000297

the reaction of benzophenone-4,4'-dicarboxylic acid and N-substitute-thiosemicarbazide derivatives with each other. After that, some biological properties of the compounds such as antibiofilm, antimicrobial, and efflux pump inhibiting efficiencies were evaluated. The absorption-emission spectra of the compounds were examined and their electrochemical properties were determined. In addition; absorption, distribution, metabolism, excretion, and toxicity (ADMET) scores were predicted by using the pharmacokinetic properties of all compounds.

MATERIAL AND METHODS

Materials

All reagents were gotten from commercial suppliers. All solvents used in synthesis and purification steps are analytical reagent-grade (Merck, Darmstadt, Germany, and Sigma-Aldrich, USA). Benzophenone-4,4'-dicarboxylic acid was gotten from TCI chemicals. Phosphorous oxychloride (99%) was obtained from Merck. Tetrabutylammonium hexafluorophosphate (TBAPF6) was provided from Aldrich. N-substitute-thiosemicarbazide derivatives were obtained as seen in the literature (25).

Instrumentation

It was used for enstrumental analysis follows: Stuart SMP10 apparatus (For Melting points); Shimadzu UV Mini-1240 UV-Vis spectrophotometer (For absorption analysis DMSO was used as solvent); Alpha FT-IR spectrometer Bruker (For FTIR analysis); Alpha FT-IR spectrometer Bruker (For ^{1}H and ^{13}C-NMR analysis); the Perkin Elmer LS55 fluorescence spectrometer (For Emission spectra).

General procedure for the synthesis of new 1,3,4-thiadiazole derivatives

4,4'-benzophenonedicarboxylic acid (1 g, 0.0037 mol, nmol), thiosemicarbazide derivative (0.0074 mol, 2n mol), and $POCl_3$ (0.0222 mol, 6n mol) were stirred under reflux for 4 hours at 90 °C. The cooled product precipitated with ice water. The neutralized mixture with ammonia solution was left in the refrigerator overnight. Final material was filtered and washed, then dried using a vacuum oven and crystallized in DMF/water (2:1) mixture. Other compounds were performed using the same procedure. Thiosemicarbazide derivatives were obtained as seen in the literature. The synthesis scheme is given in Fig 1.

Bis(4-(5-(N-cyclohexylamino)-1,3,4-thiadiazol-2-yl) phenyl)methanone (C1)

This compound was obtained as a light yellow solid. Yield: (67%), melting point (mp): 175 °C; ATR-FTIR (ν/cm^{-1}): 3200.05 (stretching, -NH); 3051.67 (Ar-H); 2926.65, 2852.56 (Aliph.-H); 1656.43 (-C=O-); 1603.05 (-C=N-); 706.88 (-C-S-C-). ^{1}H-NMR (300 MHz, DMSO-d6, δ/ppm): 8.16-7.83 (8H, Aromatic C-H); 6.97-7.29 (2H, N-H); 3.73-1.21 (22H, Aliphatic C-H in cyclohexyl). ^{13}C NMR (DMSO-d6): C-19 (194.61), C-4 and C-23 (168.84), C-1 and C-21 (154.72), C-7 and C-17 (137.54), C-12 and C-14 (135.09), C-8, C-9, C-15 and C-18 (131.06), C-10, C-11, C-13 and C-16 (126.70), C-27 and C-33 (54.14), C-28, C-29, C-34 and C-35 (32.65), C-32 and C-38 (25.67), C-30, C-31, C-36 and C-37 (24.74) (NMR details are shown in Supplementary file). Elemental analysis: (% calculated/found) for $C_{29}H_{32}N_6OS_2$ (Mw: 544.73) C: 63.94/63.37; H: 5.92/5.98; N:15.43/15.67

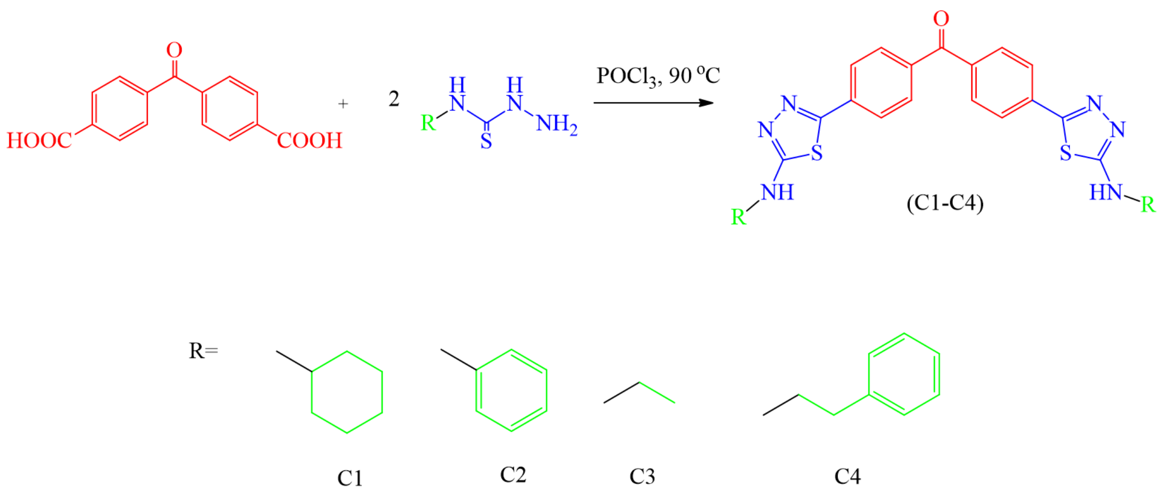

Figure 1. Synthesis route of compounds

Gur M. et al/ Hittite J Sci Eng, 2023, 10 (2) 99–116

Bis(4-(5-(N-phenylamino)-1,3,4-thiadiazol-2-yl)phenyl) methanone (C2)

Dark brown powder. Yield: (71%), melting point (mp):186 °C; ATR-FTIR (ν/cm^{-1}): 3294.82, 3194.49 (stretching, -NH); 2981.85 (Ar C-H); 1655.41 (-C=O-); 1596.78 (-C=N-); 686.66 (-C-S-C-). ^{1}H-NMR (300 MHz, DMSO-d6, δ/ppm): 8.35-6.83 (18H, Aromatic C-H); 6.08-6.73 (2H, N-H). ^{13}C NMR (DMSO-d6): C-19 (198.61), C-4 and C-23 (152.34), C-1 and C21 (167.97), C-7 and C-17 (139.24), C-12 and C-14 (138.17), C-8, C-9, C-15 and C-18 (129.16), C-10, C-11, C-13 and C-16 (128.78), C-27 and C-33 (140.54), C-28, C-29, C-34 and C-35 (117.36), C-32 and C-38 (122.57), C-30, C-31, C-36 and C-37 (129.34) (NMR details are shown in Supplementary file). Elemental analysis: (% calculated/found) for $C_{30}H_{21}N_6OS_2$ (Mw: 545.65) C: 66.03/65.92; H: 3.88/3.93; N:15.40/15.58.

Bis(4-(5-(N-ethylamino)-1,3,4-thiadiazol-2-yl)phenyl) methanone (C3)

This compound was obtained as a light brown solid. Yield: (63%), melting point (mp): 225 °C; ATR-FTIR (ν/cm^{-1}): 3212.02 (stretching, -NH); 3107.54, 2981.68 (Ar-H); 2869.55 (Aliph. C-H); 1643.23 (-C=O-); 1602.10 (-C=N-); 709.19 (-C-S-C-). ^{1}H-NMR (300 MHz, DMSO-d6, δ/ppm): 8.20-7.87 (8H, Aromatic C-H and 2H, –NH); 0.84-1.58 (10H, Aliphatic -CH_2-CH_3). ^{13}C NMR (DMSO-d6): C-19 (193.93), C-4 and C-23 (169.67), C-1 and C-21 (165.31), C-7 and C-17 (131.36), C-12 and C-14 (130.23), C-8, C-9, C-15 and C-18 (128.35), C-10, C-11, C-13 and C-16 (126.70), C-27 and C-29 (14.40), C-28 and C-30 (5.69) (NMR details are shown in Supplementary file). Elemental analysis: (% calculated/found) for $C_{211}H_{20}N_6OS_2$ (Mw 436.55) C: 57.78/57.43; H: 4.62/4.84; N:19.25/19.57.

Bis(4-(5-(N-phenethylamino)-1,3,4-thiadiazol-2-yl) phenyl)methanone (C4)

This compound was obtained as a light yellow. Yield: (%65), melting point (mp): 270 °C; ATR-FTIR (ν/cm^{-1}): 3187.89 (stretching, -NH); 2981.77 (Ar C-H); 2930.37, 28670.15 (Aliph. C-H); 1649.22 (-C=O-); 1537.69 (-C=N-); 719.12 (-C-S-C-). ^{1}H-NMR (300 MHz, DMSO-d6, δ/ppm):8.16-7.13 (18H, Aromatic C-H); 6.98-7.13 (2H, -NH); 2.79-3.01 (8H, Aliphatic -CH_2-CH_2-). ^{13}C NMR (DMSO-d6): C-19 (201.52), C-4 and C-23 (166.96), C-1 and C21 (155.24), C-7 and C-17 (139.47), C-31 and C37 (137.59), C-12 and C-14 (131.06), C-34, C-35, C-40 and C-41 (130.30), C-32, C-33, C-36 and C-39 (129.96), C-8, C-9, C-15 and C-18 (129.24), C-10, C-11, C-13 and C-16 (128.87), C-36 and C-42 (126.76), C-27 and C-28 (46.47), C-29 and C-30 (35.06) (NMR details are shown in Supplementary file). Elemental analysis: (% calculated/found) for $C_{33}H_{28}N_6OS_2$ (Mw 588.74) C: 67.32/67.43; H: 4.79/4.62; N:14.27/14.35.

Determination of antimicrobial activity

Microorganisms

The 1,3,4-thiadiazole compounds were investigated for antimicrobial activity against three microorganisms, namely *Candida albicans* DSMZ 1386, *Escherichia coli* (MDR), and *Klebsiella pneumoniae* (MDR). The strains used in this study were previously tested for their biofilm production capacities and efflux pump activities (24).

Preparing stock test solutions

1,3,4-thiadiazole compounds were dissolved in DMSO (Merck, Germany) to prepare 20 mM stock test solutions. In order to keep the final DMSO concentration below 1% in antimicrobial, antibiofilm, and efflux pump inhibition tests, the stock test solutions were diluted (26).

Preparation of the inocula

C. albicans was incubated at 27 °C for 48 hours and *E. coli*, and *K. pneumoniae* were incubated (at 37 °C for 24 hours). To prepare the inocula of the microorganisms, colonies, which were developed after incubation, were collected and suspended in 0.9% sterile saline solution until the turbidity of the inocula was equal to 0.5 Mc Farland standard (27).

Minimum inhibition concentration (MIC) test

A broth microdilution test was used for the MIC test, in which serial 2-fold dilutions were obtained in a 96-well plate in triplicates (28). The lowest compound concentration that inhibits visible microbial growth was defined as the MIC value.

Minimum bactericidal/fungicidal concentration (MBC/MFC) test

The contents of wells, in which the visible microbial growth was inhibited, were further transferred to a suitable agar medium to observe the lowest compound concentration that reduces the viability of the initial inoculum higher than 99.9%, and this concentration was defined as the MBC/MFC value (29).

Positive and negative controls

1% DMSO was used as a negative control, and gentamicin (GEN), tobramycin (TOB), and ciprofloxacin (CPFX) were positive controls.

Determination of antibiofilm activity

Determination of optimum biofilm-forming conditions

The optimum incubation time was determined by testing 24 and 48 hours for all microorganisms and optimum glucose-containing culture media was obtained by testing different glucose concentrations ranging between 0.00 and 1.25% (30).

Antibiofilm test

In antibiofilm test, compounds were used at MIC/2 concentrations. All bacteria were incubated at 37 °C and *C. albicans* at 27 °C with optimum biofilm-forming conditions obtained from the previous step (48 hours and 0.5% glucose-containing culture media) as five replicates. After the incubation period, the plates were washed with sterile distilled water (sdH_2O) several times and air-dried at 25 °C. When the plates were dried, 1 % (w/v) crystal violet solution was transferred into the wells, and the plates were re-incubated for 30 minutes at 25°C (31). The plates were washed by sdH2O and air-dried again. An ethanol-acetone (70:30 (v/v)) solution was added to each well and incubated at room temperature for 30 minutes to dissolve the crystal violet remaining in the biofilm layer. Lastly, the content of each well was transferred into a blank plate, the absorptions of each well were recorded at 595 nm by a plate reader (BioTek) (32).

Positive and negative controls

A well containing a culture medium was used as a negative control and Halamid® as a positive control.

Investigation of efflux pump inhibition activity

Ethidium bromide cartwheel test

To determine the efflux pump inhibition activity, the ethidium bromide (EtBr) cartwheel test previously defined by Martins et al was used (33). TSB agar plates containing 0.0, 0.5, 1.0, 1.5, 2.0, and 2.5 mg/L EtBr (Merck) were tested to observe the highest EtBr concentration, which can be effluxed out by each microorganism. To do that, the inocula, which was prepared as it was described previously, were transferred to EtBr containing agars and incubated under optimum conditions. After incubation, the highest EtBr concentrations effluxed out by each microorganism were distinguished by exposing EtBr containing TSB agar plates to UV light (33).

EtBr cartwheel test based efflux pump inhibition assay

TSB agar plates containing 0.5 mg/L EtBr, which was determined from the previous test, were used in this assay for all microorganisms. Tested compounds were joined to TSB plates at MIC/2 concentrations (34). The incubated plates were observed under UV light, whether tested compounds presented efflux pump inhibition activities, or not.

Positive and negative controls

TSB agar plate containing only 0.5 mg/L EtBr was used as a negative control and thioridazine hydrochloride (Sigma Aldrich), a commercial efflux pump inhibitor, as a positive control.

Drug-likeness evaluation

The drug-likeness of all 1,3,4-thiadiazole compounds were evaluated by using DruLiTo software (35) and SWISSADME server (36) according to Lipinski's (Pfizer) (37), Ghose (Amgen) (38), Veber (GSK) (39), Egan (Pharmacia) (40), and Muegge (Bayer) (41) methods by using their structural and physicochemical properties.

ADMET Analysis

Absorption, excretion, metabolism, distribution, and toxicity (ADMET) scores were predicted by using the pharmacokinetic properties of all 1,3,4-thiadiazole compounds.

By using four different tools, namely, ADMETLab server (42), admetSAR (43, 44), PreADMET (45, 46), and SWISSADME (36), some parameters like human oral bioavailability (HOB), human intestinal absorption (HIA), plasma protein binding (PPB), Caco-2 permeability, blood-brain barrier penetration (BBB), p-glycoprotein substrate/inhibitor, renal organic cation transporter (OCT2), cytochrome p450 (CYP450) substrate/inhibitor, half-time, renal clearance, drug-induced liver injury (DILI), human ether-a-go-go-related gene (hERG) inhibition, acute oral toxicity, eye injury & eye corrosion, AMES toxicity, and carcinogenicity assays were predicted.

QSAR analysis of antimicrobial activity

In QSAR analysis the numerical descriptors, which were given in Table 1, were used to identify the physicochemical properties of 1,3,4-thiadiazole compounds.

Gur M. et al/ Hittite J Sci Eng, 2023, 10 (2) 99–116

Table 1. The descriptors for QSAR analysis.

MW	Molecular waight
Volume	Van der Waals volume
logP	Log of the octanol/water partition coefficient
logS	Log of aqueous solubility
Dipole	The calculated dipole moment
EA	Electron Affinity (eV)
nHA	Number of hydrogen bond acceptors
nHD	Number of hydrogen bond donors
TPSA	Topological polar surface area
PSA	Van der Waals surface area of polar nitrogen and oxygen atoms
SASA	Total solvent accessible surface area
PISA	Carbon Pi SASA
WPSA	Weak Polar SASA
FISA	Hydrophilic SASA
FOSA	Hydrophobic SASA

Suitable descriptors for the QSAR equations were determined by Pearson's correlation matrix, and multiple linear regression (MLR) test was used for constructing QSAR models. 0.500 was selected as the limit for correlation as mentioned previously by Datar for excepting the descriptors from MLR tests (47).

Statistical analysis

All studies were conducted either in triplicates or in five replicates as mentioned above. R Studio, version 1.3.1093 was used to conduct a one-way analysis of variance (ANOVA) to obtain the results (P = 0.05) (48).

RESULTS AND DISCUSSION

The synthesis route for the compounds is presented in Experimental Section Figure 1. The compounds were obtained from 4,4'-carbonyldibenzoic acid (benzophenone-4,4'-dicarboxylic acid) and N-(substituted)-thiosemicarbazide derivatives (presence with aromatic and aliphatic groups). The compounds were obtained in good yields. Experimental and structural data of the compounds are given in the supplementary file.

Spectroscopic data

The FT-IR values of all molecules are summarized in Table 2. FT-IR bands arising from –NH vibrations are obtained at 3187.89-3294.82 cm^{-1}. vmax values; aromatic C–H peaks are seen between 2981.68-3107.54 cm^{-1}, aliphatic C–H peaks are seen at 2852.56-2930.37 cm^{-1}. –C=O– peaks are seen between 1643.23-1656.43 cm^{-1}, 1537.69-1603.05 cm^{-1} C=N peaks on the thiadiazole structure, 686.66-719.12 cm-1 peaks C–S–C for all the compounds. FT-IR spectra of all compounds are given in Supplementary File (Fig. 1-4).

The ^{1}H-NMR values of all compounds are given in Table 3. The peaks of aliphatic protons in the structures of the compounds are in the range of 0.89-3.73 ppm. While the peaks of aromatic protons are seen in the range of 6.83-8.35 ppm, the N–H protons are observed broadly in the range of 6.08-8.20 ppm. It is understood from the spectroscopic results that the resonance integration of H atoms in the structures is compatible with the structures.

Table 2. FT-IR results for all compounds

Compounds	(u, cm^{-1})					
	u(-NH)	uC-H (Aromatic)	uC-H (Aliphatic)	u(C=O)	u(C=N)	u(C-S-C)
C1	3200.05	2981.85	2926.65 2852.56	1656.43	1603.05	706.88
C2	3294.82 3194.49	3051.67	-	1655.41	1596.78	686.66
C3	3212.02	3107.54 2981.68	2869.55	1643.23	1602.10	709.19
C4	3187.89	2981.77	2930.37 2870.15	1649.22	1537.69	719.12

Table 3. ^{1}H-NMR results for all compounds

Compounds	(δ,ppm)		
	δ(Aliphatic C-H)	δ(Aromatic C-H)	δ(N-H)
C1	1.21-3.73 (22 H, cyclohexyl C-H)	7.83-8.16 (8H, phenyl C-H)	6.97-7.29
C2	-	6.83-8.35 (18H, phenyl C-H)	6.08-6.73
C3	0.84-1.58 (10 H, $-CH_2-CH_3$)	7.87-8.20 (8H, phenyl C-H)	7.87-8.20
C4	2.79-3.01 (8H, $-CH_2-CH_2-$)	7.13-8.16 (18H, phenyl C-H)	6.98-7.13

Absorption and fluorescence studies

The absorption and fluorescence spectra of the compounds (C1-C4) were obtained in DMSO and the corresponding data were given in Table 4 (Concentrations of synthesized compounds were prepared in the range of 10^{-4}-10^{-5} M). The UV-Vis spectra of C1-C4 show a band between 325 nm and 351 nm due to the n→π* transitions of the carbonyl group of benzophenone.

The fluorescence spectra of C1-C4 show emission wavelengths in the range 490 nm and 504 nm which give blue emission colour (Figure 2). The emission band of C3 with ethyl substituents exhibits red-shifted compared to C1, C2, and C4 with cyclohexyl, phenyl, and 2-phenylethyl substituents. The electron donor property of ethyl substituent can stabilize the LUMO energy level of the compounds, leading to the redshift of emission wavelength (25). The emission intensity of C3 increases in the presence of ethyl substituents at 1,3,4-thiadiazole-2-amine when comparing the molecules with other substituents. The obtained results indicate that the substituents of the compounds have an important effect on the absorption (49) and fluorescence properties.

Electrochemical data

The electrochemical studies were conducted using cyclic voltammetry in 0.1 M TBAPF6 in DMSO as a supporting electrolyte. The electrochemical data were summarized in Table 4. The compounds (C1-C4) show one oxidation peak in the range of 1.32 V and 1.46 V due to thiadiazole fragments of the molecules (Figure 3a) (25).

The HOMO energy levels of C1-C4 were determined using the oxidation potential of the compounds and ferrocene as an internal standard (E1/2(Fe) = 0.60 V vs. Ag/Ag+) (EHOMO = -e(E1/2(ox.,dye) - E1/2(Fe) + 4.8) (50). The LUMO energy levels of the C1-C4 were calculated with the equation, ELUMO = EHOMO + Eg, (50). The calculated HOMO and LUMO energy levels are between (-5.52) to (-5.66) eV and (-2.56) to (-2.71) eV, respectively. The electrochemical characterizations of molecules are significant for bioactivity, biofilm, and molecules-bacteria interaction (51, 52). The electrochemical stability of molecules plays an important role in biofilms which are used in the photosynthetic plasmonic voltaic device (53) and energy batteries (54). In the consecutive cyclic voltammograms of C1-C4, no significant changes in peak currents and potentials are observed (Figure 3b). This indicates that the compounds have electrochemical stability.

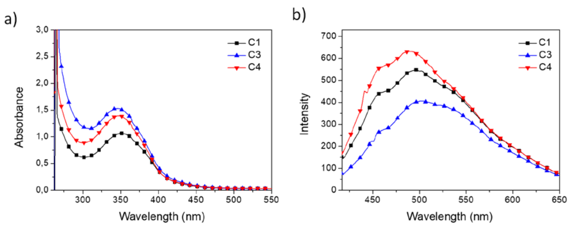

Figure 2. The absorption (a) and emission (b) spectra of C1, C3, C4.

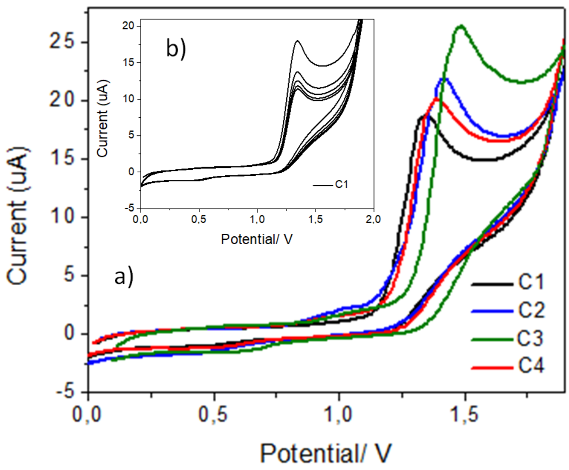

Figure 3. a) The cyclic voltammograms of C1, C2, C3 ve C4, b) The consecutive cyclic voltammograms of C1.

Table 4. The absorption, emission, and electrochemical data of C1-C4.

Compounds	λ_{max}^{Abs} (nm)	λ_{max}^{Em} (nm)	E_{ox} (V)	Band Gap (eV)	HOMO (eV)	LUMO (eV)
C1	351	496	1.32	2.96	-5.52	-2.56
C2	325	500	1.39	3.01	-5.59	-2.58
C3	346	504	1.46	2.95	-5.66	-2.71
C4	348	490	1.37	2.94	-5.57	-2.63

MIC and MBC/MFC tests results

MIC values for all 1,3,4-thiadiazole compounds and positive control antibiotics (GEN, TOB, and CPFX) against *C. albicans*, *E. coli*, and *K. pneumoniae* are given in Table 5.

The results of the MIC test, which are not given in Table 5, showed that negative control (1% DMSO) had no activity on any of the microorganisms.

Table 5. MIC test results (µg/mL)

	C1	C2	C3	C4	GEN	TOB	CPFX
C. albicans	3.77	0.91	2.68	4.21	10.00	NA	NA
E. coli	3.77	NA	2.68	NA	NA	NA	NA
K. pneumonia	15.08	7.30	NA	NA	2.50	2.50	0.08

"NA": No Activity.

The results showed that only GEN had activity on *C. albicans* with a MIC value of 10.00 µg/mL, and all positive control antibiotics (GEN, TOB, and CPFX) presented activity against *K. pneumoniae* with MIC values of 2.50, 2.50, and 0.08 µg/mL respectively. According to the MIC test results, all compounds presented higher antibacterial activity compared to all positive control antibiotics. In addition, C1 and C2 showed antibacterial activity against *K. pneumoniae*, but the MIC values are higher than GEN, TOB, and CPFX.

On the other hand, any positive control antibiotics did not show activity on *E. coli*, but C1 and C3 presented relatively high antibacterial activities.

Several researchers have published studies until now about the antimicrobial results of 1,3,4-thiadiazole derivatives. In one of the studies, the antimicrobial properties of some the compounds were tried against several microorganisms including *C. albicans* ATCC 10231, and *E. coli* ATCC 25922. Accordingly, these compounds were observed to be only active against *C. albicans* among these three strains (55). In another study, several 1,3,4-thiadiazole derivatives were tested for their antibacterial and antifungal properties in several microorganisms including *E. coli* ATCC 25922, but these compounds presented no activity against *E. coli* (56). Another research observed either no activity, weak or moderate activities of some 1,3,4-thiadiazole derivatives on

E. coli (57). One of the previous studies published by our group presents that some of these derivatives had antimicrobial activities against *C. albicans*, and *K. pneumoniae*, but none of them were active against *E. coli*, which were the same strains used in this present study (24). These studies reveal that the results on the subject of the antibacterial and antifungal effects of the 1,3,4-thiadiazole derivatives were conflicting. The dissimilarities regarding the antibacterial and antifungal activities are mainly due to the differences in the strains used in different studies and the atoms attached to the main structure of the 1,3,4-thiadiazole derivatives.

Antibiofilm tests results

According to the antibiofilm tests, the compounds tested in this study showed dose-dependent activities, such as some concentrations activated biofilm formation, whereas some others inactivated.

In the Table 6, it was presented the maximum inhibition percentages in biofilm with a minimum 1,3,4-thiadiazole derivative concentration. The antibiofilm tests revealed that the compounds presented an antibiofilm effect on all the bacteria tested, where no activity was observed on *C. albicans.*

Table 6. The maximum inhibition percentages in biofilm with a minimum 1,3,4-thiadiazole derivative concentration

	C1	C2	C3	C4	Halamid®
C. albicans	-	-	-	-	69 % (1.95 μg/mL)
E. coli	10 % (3.77 μg/mL)	32 % (1.83 μg/mL)	6 % (1.34 μg/mL)	12 % (0.13 μg/mL)	46 % (0.41 μg/mL)
K. pneumonia	100 % (0.12 μg/mL)	52 % (0.11 μg/mL)	25 % (0.08 μg/mL)	33 % (0.13 μg/mL)	53 % (0.41 μg/mL)

"-": No inhibition observed.

The percentages of the biofilm inhibition of the test compounds on *E. coli* were calculated to be between 6 and 32 %, which were lower than the activity of Halamid®.

According to the results, C1 was observed to inhibit 100% of biofilm formation in *K. pneumoniae*, whereas Halamid® could only inhibit 53 % of biofilm formation. In addition, C2 inhibited 52 % of biofilm formation, which was quite close to the activity of Halamid®.

Biofilms are known to be the main reason for the infectious diseases generally linked to Foley catheters, cerebrospinal shunts, and vascular catheters (58–61). Furthermore, they cause several health problems in some tissues, such as the skin, urinary tract, and teeth (62, 63). In biofilm-forming microorganisms, biofilms also play an important role in increasing resistance to antibiotics or antifungal agents (64). For this reason, inhibiting the formation of biofilms has great importance in both the industry and public health. Looking at Table 6, it appears that some of the test compounds have promising antibiofilm potential on the tested microorganisms.

There are several studies in the literature proving that 1,3,4-thiadiazole derivatives possibly inhibit biofilm formation. One of these studies also tested some 1,3,4-thiadiazole compounds on *E. coli* ATCC 25922. As a result, they proposed that some 3,4-thiadiazole derivatives presented antibiofilm activities on these strains (65).

In another study, it was concluded that some benzothiophene and indole derivatives had biofilm inhibiting activities on *E. coli* and MRSA too (66).

One of our previous studies proved that nearly all of the 1,3,4-thiadiazole compounds had biofilm inhibiting activities against *C. albicans*, *E. coli*, and *K. pneumoniae*, but the inhibition percentages in *K. pneumoniae* were observed to be better in this present study (24).

In addition to biofilm inhibiting activities, the test compounds were observed to present dose-dependent biofilm activating properties. Table 7 shows the maximum activation percentages in biofilm with a minimum 1,3,4-thiadiazole derivative concentration.

Table 7. The highest biofilm activation percentages (%) with the lowest compound concentrations (μg/mL)

	C1	C2	C3	C4
C. albicans	49 % (0.24 μg/mL)	47 % (0.23 μg/mL)	45 % (0.17 μg/mL)	35 % (4.21 μg/mL)
E. coli	17 % (0.94 μg/mL)	9 % (0.46 μg/mL)	11 % (0.34 μg/mL)	-
K. pneumonia	5 % (0.94 μg/mL)	11 % (0.46 μg/mL)	4 % (0.17 μg/mL)	-

"-": No inhibition observed.

The results showed that all compounds triggered biofilm formation between 35 and 49 % in *C. albicans*. For *E. coli* and *K. pneumoniae*, all compounds except C4 were observed to trigger biofilm formation with relatively lower percentages, which were between 9 and 17 % for *E. coli* and between 4 and 11 % for *K. pneumoniae*.

Some studies in the literature proved that 1,3,4-thiadiazole derivatives may promote biofilm formation. One of these studies demonstrated that some 1,3,4-thiadiazole indole and benzothiophene derivatives stimulated biofilm formation by 50% in *E. coli* (66).

One of our recent studies confirmed that 1,3,4-thiadiazole derivatives may trigger biofilm formation in *C. albicans*, *E. coli*, and *K. pneumoniae* (24).

Gur M. et al/ Hittite J Sci Eng, 2023, 10 (2) 99–116

Biofilms have several practical uses to progress some beneficial products, such as foods for animals, input for biofuel production, high valuable chemicals, pharmaceuticals, and bioplastics (67, 68). Biofilms are also used in photosynthetic plasmonic voltaic devices to produce electrical power (53). Moreover, some other studies proved that biofilms can be used in high power and high energy batteries to coat separators (54). This study also verified that biofilm-covered nanofibers have the potential of enhancing adhesions between electrodes and separators. In addition, they improve electrolytes to maintain solid-liquid interactions and the number of lithium transference. According to this perspective, activating the production of biofilms could have some benefits.

Efflux pump inhibiting test results

In the efflux pump inhibiting test, all compounds were joined into TSB plates containing 0.5 mg/L EtBr with subinhibitory concentrations (MIC/2). Results of the efflux pump inhibiting test presented that the 1,3,4-thiadiazole compounds inhibited the activities of efflux pumps in some of the microorganisms and EtBr reacted with nucleic acids and cause fluorescence. But no fluorescence was observed in negative control plates, but in all bacteria and *C. albicans* the positive control plates containing thioridazine hydrochloride triggered fluorescence. The results given in Table 8 showed that C2 and C3 inhibited efflux pump activity in *K. pneumoniae* and C4 in *E. coli*. On the other hand, none of the compounds caused an inhibition in *C. albicans*.

Table 8. Efflux pump inhibition

	C1	C2	C3	C4
C. albicans	-	-	-	-
E. coli	-	-	-	+
K. pneumonia	-	+	+	-

"+": Inhibition observed."-": No inhibition observed.

Since efflux pumps are important in obtaining antibiotic resistance, inhibition of efflux pumps could help prevent the development of antibiotic resistance (69). As a result of this, the results of the efflux pump inhibition test are quite promising.

Several researchers also previously tested the efflux pump inhibiting activities of some 1,3,4-thiadiazole derivatives. One of these studies proved that some 1,3,4-thiadiazole derivatives caused antimicrobial activity by inhibiting efflux pumps in *E. coli*, and *C. albicans* (70).

A group of researchers synthesized some 3-nitro-6-amino-indole and 3-amino-6-carboxyl-indole derivatives specifically to bind and inhibit the TolC type efflux pumps. As a result, they observed that these compounds decreased MIC values of ciprofloxacin, erythromycin, tetracycline, and chloramphenicol by 2 to 64 folds in two different *E. coli* strains (71). However, some researchers presented that indole derivatives activated efflux pump types of ramA and acrAB in Salmonella Typhimurium (72) and TtgGHI in Pseudomonas putida (73) and as a result, they caused an increased antibiotic resistance.

Druglikeness results

The clinical research steps of testing any drug candidate are long, exhausting, and expensive. Thus, any candidate compound having promising results in the pre-clinical research should be evaluated regarding its druglikeness properties before conducting further clinical research. In resulting the druglikeness properties of a candidate compound several chemical and physicochemical properties are taken into account. Lipinski's, Ghose, Veber, Egan, and Muegge approaches are the common methods to define the druglikeness properties of any candidate compound. The number of druglikeness violations of 1,3,4-thiadiazole compounds are given in Table 9.

Table 9 presents that only C3 fulfilled Lipinski's druglikeness rules, but some violations were observed according to other approaches. On the other hand, other compounds have violations for all druglikeness approaches. Lipinski's is the most common approach in defining the druglikeness properties of target compounds. In addition, most of the values causing violations according to other approaches are very close to the limits. Thus, it is possible to propose that C3 has a drug-like nature.

Fig. 4 shows that all 1,3,4-thiadiazole derivatives other than C3 are out of the colored zone. But C3 is very close to the colored zone, which presents its oral availability potential.

ADMET Analysis

The pharmacokinetic properties and ADMET (absorption, excretion, distribution, metabolism and toxicity) profiles of test compounds were calculated by admetSAR, SWISSADME, PreADMET, and pharmacokinetic properties were screened by ADMETLab server. The data were presented in Table 10.

There are several parameters that can be used to obtain the absorption of drug candidates. In this study, the human intestinal absorption (HIA), Madin-Darby canine kidney (MDCK) cell permeability and Caco-2 permeability parameters, which are commonly used tools to evaluate membrane permeability screening (74,75), were selected. The

Table 9. Drug property screening results of 1,3,4-thiadiazole derivatives.

Physicochemical Characterizations

	MW (mw)	MLogP	XLOGP3	WLogP	H-Bond Acceptor	H-Bond Donor	TPSA	AMR	RB (nRB)	NoA
C1	544.73	4.23	7.73	7.06	5	2	149.17	156.58	8	70
C2	532.64	4.36	7.23	7.44	5	2	149.17	153.21	8	58
C3	464.61	3.01	5.9	5.22	5	2	149.17	131.96	10	56
C4	588.75	4.58	8.02	6.88	5	2	149.17	171.32	12	70

Druglikeness Violations

	Lipinski's (Pfizer)	Ghose (Amgen)	Veber (GSK)	Egan (Pharmacia)	Muegge (Bayer)	Bioava-ilability Score
C1	2: MW>500, MLOGP>4.15	3: MW>480, WLOGP>5.6, MR>130	1: TPSA>140	2: WLOGP>5.88, TPSA>131.6	1: XLOGP3>5	0.17
C2	2: MW>500, MLOGP>4.15	3: MW>480, WLOGP>5.6, MR>130	1: TPSA>140	2: WLOGP>5.88, TPSA>131.6	1: XLOGP3>5	0.17
C3	0	1: MR>130	1: TPSA>140	1: TPSA>131.6	1: XLOGP3>5	0.55
C4	2: MW>500, MLOGP>4.15	3: MW>480, WLOGP>5.6, MR>130	2: Rotors>10, TPSA>140	2: WLOGP>5.88, TPSA>131.6	1: XLOGP3>5	0.17

MW: Molecular weight, **TPSA:** Total Polar Surface Area, **AMR:** Atom Molar Refractivity, **RB:** Rotable Bond, **NoA:** Number of Atom

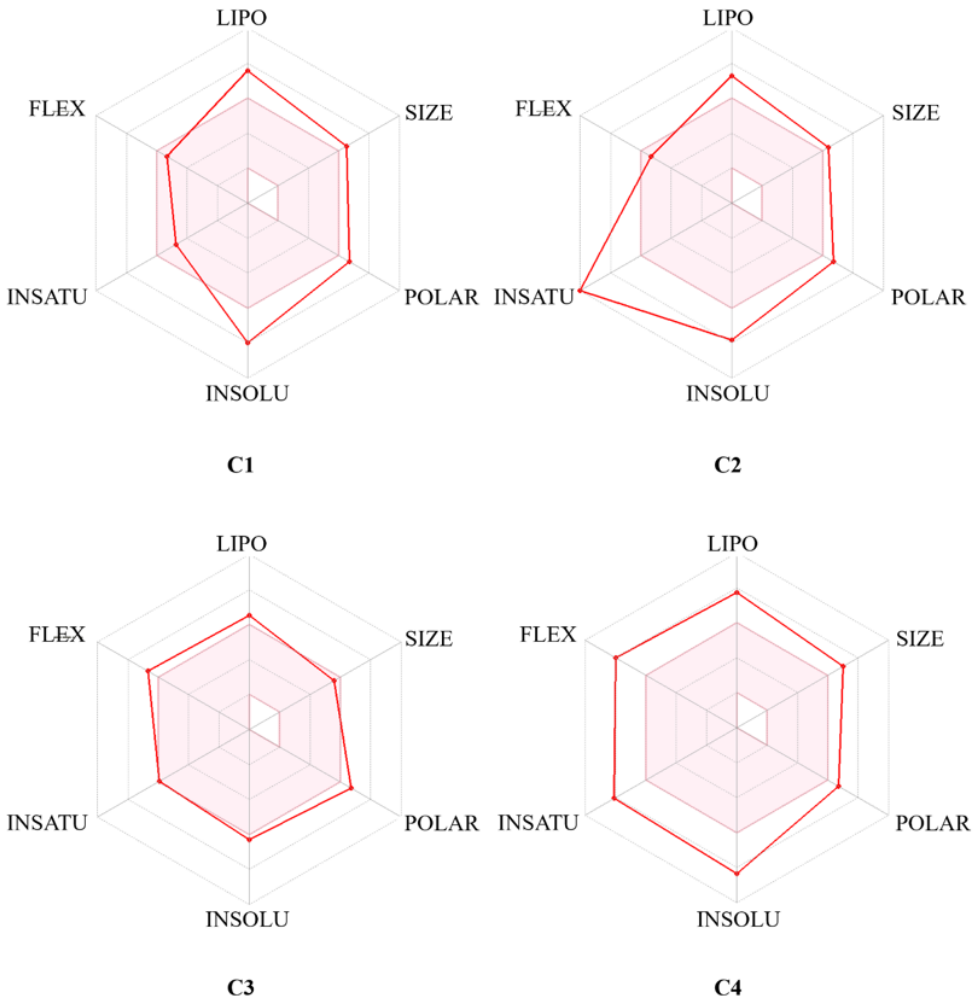

Figure 4. The graphs regarding the quality of being efficacious when taken by mouth (oral availability) for 1,3,4-thiadiazole derivatives. (* Size (SIZE), polarity (POLAR), insolubility (INSOLU), insaturation (INSATU), flexibility (FLEX), and lipophilicity (LIPO))

Table 10. ADMET profiles for 1,3,4-thiadiazole derivatives.

	C1	C2	C3	C4
1. Absorption				
Human intestinal absorption (%)	HIA+	HIA-	HIA+	HIA-
MDCK Permeability (cm/s)	3.4e-05	1.6e-05	2.8e-05	2.7e-05
Caco-2 permeability (Log Unit)	-4.49	-4.616	-4.132	-4.670
2. Distribution				
Plasma protein binding (%)	98.718	100.400	96.728	100.106
P-glycoprotein substrate	Yes	No	Yes	Yes
P-glycoprotein inhibitor	Yes	Yes	Yes	Yes
Blood-brain barrier penetration	BBB+	BBB+	BBB+	BBB-
Volume distribution (L/kg)	1.477	0.805	1.557	1.241
The fraction unbound in plasma (%)	0.335	0.299	2.118	0.345
3. Metabolism				
CYP450 2C9 Substrate	No	Yes	No	No
CYP450 2D6 Substrate	No	No	No	No
CYP450 2C19 Substrate	No	No	No	No
CYP450 3A4 Substrate	No	No	No	No
CYP450 1A2 Substrate	No	No	Yes	No
CYP450 2C9 Inhibitor	Yes	Yes	Yes	Yes
CYP450 2D6 Inhibitor	Yes	No	Yes	Yes
CYP450 2C19 Inhibitor	Yes	Yes	Yes	Yes
CYP450 3A4 Inhibitor	Yes	Yes	Yes	Yes
CYP450 1A2 Inhibitor	Yes	Yes	Yes	Yes
4. Excretion				
Half-time (t1/2) (h)	0.002	0.01	0.011	0.005
Renal clearance (mL/min/kg)	1.026	0.697	1.157	1.273
5. Toxicity				
Organ Toxicity				
Drug-induced liver injury	DILI+	DILI+	DILI+	DILI+
hERG inhibition	hERG +	hERG -	hERG +	hERG +
Acute oral toxicity	-	-	-	-
Eye injury & eye corrosion	No	No	No	No
Genomic Toxicity				
AMES toxicity	AMES+	AMES+	AMES-	AMES+
Carcinogenicity	+	+	+	-

results about the absorption of the compounds confirmed that C1 and C3 are in an acceptable range for all absorption parameters, thus it is possible to accept them as efficient drug candidates, but C2 and C4 have problems only for HIA. All 1,3,4-thiadiazole compounds presented acceptable results both for MDCK permeability and Caco-2 permeability. These results present that passive diffusion through the epithelium of intestines is possible (74). Another important step in ADMET tests is evaluating the distribution parameters for drug candidates. In the literature, several tests were proposed to evaluate the distribution properties. In this study, plasma protein binding (PPB), P-glycoprotein substrate/inhibitor, and blood-brain barrier penetration (BBB) were chosen (43, 44). In addition to these, volume distribution and the fraction unbound in plasma data were also supported.

According to the results, C2 and C4 presented the highest PPB affinities, which were over 100%, and the lowest was for C3 at 96.728%. It was previously proposed that the drug candidates with a PPB affinity of more than 90 % show insufficient accuracy (75) and a PPB affinity exceeding 95% are recognized as having a lower therapeutic index (76), which is related to a high risk of toxicity (77). Since having high toxicity risk is a limiting problem for a therapeutic compound, it can be recommended to use a combination of compounds that help in displacing them from plasma proteins. In contrast, to keep free therapeutic compound concentrations comparatively constant, therapeutic compound-protein complexes in the blood plasma serve as a drug reservoir. This serves as an extended activity of drugs (75).

One of the efflux transporters is P-glycoproteins and they alter the ADE (absorption, distribution, and elimination) properties of drugs. These proteins especially limit the absorption of drugs through the intestines, which are delivered orally (78, 79). According to the results, all 1,3,4-thiadiazole derivatives were P-glycoprotein inhibitors.

BBB is taken into account for drugs that can be used against neurodegenerative problems. Previous studies proved that in clinical trials 98% of drugs presented inadequate BBB permeability (80, 81). Table 9 demonstrates that all compounds except C4 are BBB+. Any drug directing the central nervous system (CNS) should have BBB permeable properties (82, 83).

Plasma protein binding significantly affects the volume of distribution and the volume of distribution is sensitive to the fraction unbound in plasma. The results showed that the volume of distributions for all compounds was between 0.04 and 20 L/kg, which is accepted to be at the optimal level and the values of fraction unbound in plasma were <5%, which is low. Even though therapeutic compounds highly bound to plasma proteins restrict the concentration of the drugs in the blood plasma, hydrophobic bases which bind to α-acid glycoprotein can be highly partitioned into tissues (84, 85).

To understand how therapeutic compounds are metabolized, cytochromes P450 (CYP) studies are usually conducted. These enzymes (CYP1, CYP2, and CYP3) are the enzymes controlling the biotransformation of many drugs. In addition, they are significant in the metabolism of fatty acids too (86, 87).

The data that is given in Table 10 presents that only C2 is a substrate for CYP450 2C9 and C3 for CYP450 1A2. On the other hand, all the test compounds are inhibitors of CYP1, CYP2, and CYP3 enzymes except for C2 against CYP450 2D6.

The excretion parameters for drug candidates are also evaluated by ADMET tests. The renal clearance and half-time parameters were used for this purpose. If these values are lower than 5mL/min/kg and 3 hours respectively, Di and Kerns accepted that half-time and renal clearance are low (88). Thus, the results in Table 10 show that the renal clearances and half-times of all test compounds are low.

The last parameter used in ADMET tests is the toxicity of therapeutic compounds, and for this purpose, genomic and organ toxicity tests were applied.

Hepatotoxicity induced by therapeutic compounds is a common reason for injury in the liver. DILI (Drug-induced liver injury) is one of the significant parameters, which led to withdrawals of drugs on the market for safety reasons (89). Results showed that the test compounds used in this study were DILI+.

The hERG (human ether-a-go-go-related gene) is known to encode some potassium channels, and it is accepted that any compound inhibiting the hERG, also inhibits these potassium channels, which causes severe cardiac problems (90). According to the results, all test compounds used in this study, except C2, inhibit the hERG.

The results showed that no acute oral toxicity was observed for all the 1,3,4-thiadiazole compounds. Moreover, none of these 1,3,4-thiadiazole derivatives was observed to cause eye corrosion or eye injury.

To predict any carcinogenicity or mutagenesis possibilities at the early stages, the AMES test is applied commonly (91). The results show that (Table 10) all test compounds, except C3 were AMES positive.

Most likely, the main concern in assessing drug candidates is the carcinogenicity test to determine whether they are suitable for human health or not (92). Data obtained from this test presented that only C4 is a non-carcinogen.

QSAR analysis for antimicrobial properties

The values for the descriptors of the test compounds used for QSAR analysis are given in Table 11 (see Table 1 for descriptions of the descriptors of the QSAR analysis). Since there are some correlations between the descriptors, some of them were excluded before MLR analysis based on the limit of the correlation of 0.500, and linear QSAR equations were developed by the stepwise addition of terms (47). In order to determine the important descriptors for biofilm inhibition, antibacterial and antifungal activities of 1,3,4-thiadiazole derivatives QSAR analysis was conducted.

QSAR analysis was carried out only for *C. albicans* for antimicrobial activity, and *E. coli* and *K. pneumoniae* for biofilm inhibiting activities, since reliable MRL analysis can only be conducted for these values.

The data about the best MRL models calculated by applying stepwise regression are given in Table 12.

The QSAR results presented that TPSA (topological polar surface area) is the main descriptor important in the

Table 11. Descriptor values regarding test compounds.

Compounds	C1	C2	C3	C4
MW	544.731	532.637	436.549	588.744
Volume	6.567	6.176	4.239	7.729
logP	-10.158	-8.982	-7.139	-10.847
logS	1.072	1.538	1.524	1.308
Dipole	1.226	1.387	1.249	1.280
EA	2.000	2.000	2.000	2.000
nHA	7.000	7.000	7.000	7.000
nHD	149.170	149.170	149.170	149.170
TPSA	1702.639	1570.678	1349.072	1827.815
PSA	100.093	96.625	103.073	101.862
SASA	949.217	883.243	777.796	1023.973
PISA	270.613	666.164	271.103	660.599
WPSA	81.571	80.821	81.590	81.603
FISA	132.693	136.258	150.617	143.870
FOSA	464.339	0.000	274.486	137.901

antifungal effect of test compounds on *C. albicans* only for p= 0.100. On the other hand, WPSA (Weak Polar SASA) is the main descriptor for the biofilm inhibition effect of the test compounds on *E. coli* ($p < 0.05$) but none of the descriptors are observed to have importance for the biofilm inhibiting effect of test compounds on *K. pneumoniae*.

Table 12. Best MLR models for antimicrobial and antibiofilm activity predictions.

Antimicrobial activity						
Microorganism	**Equation**	**N**	**R2**	**Adjusted R2**	**Std. Error**	**p-Value**
C. albicans	MIC = -278.11 + 3.452 TPSA	4	0.812	0.719	0.780	0.100
Antibiofilm activity						
E. coli	Inhibition% = 24.136 - 0.295 WPSA	4	0.950	0.924	0.032	0.026

CONCLUSION

To sum up, Bis(4-(5-(N-cyclohexylamino)-1,3,4-thiadiazol-2-yl)phenyl)methanone (C1), Bis(4-(5-(N-phenylamino)-1,3,4-thiadiazol-2-yl)phenyl)methanone (C2), Bis(4-(5-(N-ethylamino)-1,3,4-thiadiazol-2-yl)phenyl)methanone (C3), and Bis(4-(5-(N-phenethylamino)-1,3,4-thiadiazol-2-yl)phenyl)methanone (C4) were synthesised. Also, their spectroscopic characterizations were conducted with FTIR, ^{1}H-NMR, and ^{13}C-NMR spectroscopic techniques with elemental analysis. Furthermore, this study cover synthesized the new four compounds and their antibiofilm, antimicrobial, efflux pump inhibiting activities, and ADMET featurities were examined in detail. The MIC test results showed that all derivatives presented better antimicrobial activity against *C. albicans* compared to GEN, and some of them had antimicrobial activity against *K. pneumoniae* and *E. coli*. But according to the MBC and MFC tests, all the antimicrobial activities of compounds were found to be bacteriostatic. Moreover, test compounds showed biofilm inhibiting or activating properties depending on the concentration. Especially the biofilm inhibition activity of C1 against *K. pneumoniae* is noteworthy. In addition, C4 was observed to exhibit efflux pump inhibition activity in *E. coli*, whereas C2 and C3 in *K. pneumoniae*. ADMET tests showed that some of these compounds have therapeutic compound potentials, nevertheless it is possible to rise toxicity concerns. Therefore, it is possible to propose to conduct additional tests to determine concentrations which are active but non-toxic. Furthermore, based on the fact that no significant changes in peak currents and potentials were observed in consecutive cyclic voltammograms of C1-C4, it can be suggested that the compounds have electrochemical stability.

ACKNOWLEDGEMENTS

The authors are grateful to the Scientific Research Projects Council of Kastamonu University (KÜ-BAP01/2019-3).

CONFLICT OF INTEREST

There is no financial conflict of interest with any institution, organization, person related to our article named "Novel 1,3,4-Thiadiazole Derivatives as Antimicrobial, Antibiofilm, Efflux Pump Inhibiting Agents and Their ADMET Properties" and there is no conflict of interest between the authors.

.

AUTHOR CONTRIBUTION

The synthesis, characterization, absorption, and emission studies were carried out by Mahmut Gur, Merve Zurnaci, Nesrin Sener, and Izzet Sener. The antimicrobial, antibiofilm, and efflux pump inhibiting activities were investigated by Eda Altinoz, Merve Senturan, and Ergin Murat Altuner, and Altuner also carried out ADMET studies.

The electrochemical properties of the compounds were studied by Çigdem Sahin. All authors reviewed the manuscript.

References

1. Janowska S, Paneth A, Wujec M. Cytotoxic Properties of 1,3,4-Thiadiazole Derivatives—A Review. Molecules 2020;25:4309. https://doi.org/10.3390/molecules25184309.
2. Ningegowda R, Shivananju NS, Rajendran P, Basappa, Rangappa KS, Chinnathambi A, et al. A novel 4,6-disubstituted-1,2,4-triazolo-1,3,4-thiadiazole derivative inhibits tumor cell invasion and potentiates the apoptotic effect of TNFα by abrogating NF-κB activation cascade. Apoptosis 2017;22:145–57. https://doi.org/10.1007/s10495-016-1312-8.
3. Lalita, Chauhan ; Shalini G. Journal of drug delivery and therapeutics (jddt). Journal of Drug Delivery & Therapeutics 2020;9:661–8.
4. Disposition D. Op Y Ig Ht S Ht S 2015;46:750–6.
5. Datar PA. Design and Synthesis of Thiadiazole Derivatives as Antidiabetic Agents. Medicinal Chemistry 2014;4. https://doi.org/10.4172/2161-0444.1000170.
6. Thrilochana, P., Sahu, C. N., Hazra, K., and Ramachandran S. Synthesis and Biological Evaluation of New Thiadiazole Analogs for Anti-diabetic Activity against Alloxan-Induced Diabetes. J Pharm Res 2014;8:1–8.
7. Cristina A, Leonte D, Vlase L, Bencze L, Imre S, Marc G, et al. Heterocycles 48. Synthesis, Characterization and Biological Evaluation of Imidazo[2,1-b][1,3,4]Thiadiazole Derivatives as Anti-Inflammatory Agents. Molecules 2018;23:2425. https://doi.org/10.3390/molecules23102425.
8. Schenone S, Brullo C, Bruno O, Bondavalli F, Ranise A, Filippelli W, et al. New 1,3,4-thiadiazole derivatives endowed with analgesic and anti-inflammatory activities. Bioorganic & Medicinal Chemistry 2006;14:1698–705. https://doi.org/10.1016/j.bmc.2005.10.064.
9. Can ÖD, Altıntop MD, Özkay ÜD, Üçel Uİ, Doğruer B, Kaplancıklı ZA. Synthesis of thiadiazole derivatives bearing hydrazone moieties and evaluation of their pharmacological effects on anxiety, depression, and nociception parameters in mice. Archives of Pharmacal Research 2012;35:659–69. https://doi.org/10.1007/s12272-012-0410-6.
10. Samel AB, Pai NR. Synthesis of Novel Aryloxy Propanoyl Thiadiazoles as Potential Antihypertensive Agents. Journal of the Chinese Chemical Society 2010;57:1327–30. https://doi.org/10.1002/jccs.201000196.
11. Serban G. Synthetic Compounds with 2-Amino-1,3,4-Thiadiazole Moiety Against Viral Infections. Molecules 2020;25:942. https://doi.org/10.3390/molecules25040942.
12. Brai, Ronzini, Riva, Botta, Zamperini, Borgini, et al. Synthesis and Antiviral Activity of Novel 1,3,4-Thiadiazole Inhibitors of DDX3X. Molecules 2019;24:3988. https://doi.org/10.3390/molecules24213988.
13. Azar Tahghighi and FB. Thiadiazoles: the appropriate pharmacological scaffolds with leishmanicidal and antimalarial activities: a review. Iran J Basic Med Sci 2017;20:613–22. https://doi.org/10.22038/IJBMS.2017.8828.
14. Sadat-Ebrahimi SE, Mirmohammadi M, Tabatabaei ZM, Arani MA, Jafari-Ashtiani S, Hashemian M, et al. Novel 5-(Nitrothiophene-2-yl)-1,3,4-thiadiazole derivatives: Synthesis and antileishmanial activity against promastigote stage of leishmania major. Iranian Journal of Pharmaceutical Research 2019;18:1816–22. https://doi.org/10.22037/ijpr.2019.14547.12476.
15. Muğlu H, Şener N, Mohammad Emsaed HA, Özkınalı S, Özkan OE, Gür M. Synthesis and characterization of 1,3,4-thiadiazole compounds derived from 4-phenoxybutyric acid for antimicrobial activities. Journal of Molecular Structure 2018;1174:151–9. https://doi.org/10.1016/j.molstruc.2018.03.116.
16. Gür M, Yerlikaya S, Şener N, Özkınalı S, Baloglu MC, Gökçe H, et al. Antiproliferative-antimicrobial properties and structural analysis of newly synthesized Schiff bases derived from some 1,3,4-thiadiazole compounds. Journal of Molecular Structure 2020;1219. https://doi.org/10.1016/j.molstruc.2020.128570.
17. Cascioferro S. The Future of Antibiotic: From the Magic Bullet to the Smart Bullet. Journal of Microbial & Biochemical Technology 2014;06. https://doi.org/10.4172/1948-5948.1000e118.
18. Cascioferro S, Cusimano MG, Schillaci D. Antiadhesion agents against Gram-positive pathogens. Future Microbiology 2014;9:1209–20. https://doi.org/10.2217/fmb.14.56.
19. Schillaci D, Spanò V, Parrino B, Carbone A, Montalbano A, Barraja P, et al. Pharmaceutical Approaches to Target Antibiotic Resistance Mechanisms. Journal of Medicinal Chemistry 2017;60:8268–97. https://doi.org/10.1021/acs.jmedchem.7b00215.
20. Lynch AS, Robertson GT. Bacterial and Fungal Biofilm Infections. Annual Review of Medicine 2008;59:415–28. https://doi.org/10.1146/annurev.med.59.110106.132000.
21. Parrino B, Diana P, Cirrincione G, Cascioferro S. Bacterial Biofilm Inhibition in the Development of Effective Anti-Virulence Strategy. The Open Medicinal Chemistry Journal 2018;12:84–7. https://doi.org/10.2174/1874104501812010084.
22. Raimondi MV, Maggio B, Raffa D, Plescia F, Cascioferro S, Cancemi G, et al. Synthesis and anti-staphylococcal activity of new 4-diazopyrazole derivatives. European Journal of Medicinal Chemistry 2012;58:64–71. https://doi.org/10.1016/j.ejmech.2012.09.041.
23. Schillaci D, Petruso S, Cascioferro S, Raimondi MV, Haagensen JAJ, Molin S. In vitro anti-Gram-positive and antistaphylococcal biofilm activity of newly halogenated pyrroles related to pyrrolomycins. International Journal of Antimicrobial Agents 2008;31:380–2. https://doi.org/10.1016/j.ijantimicag.2007.10.013.
24. Zurnacı M, Şenturan M, Şener N, Gür M, Altınöz E, Şener İ, et al. Studies on Antimicrobial, Antibiofilm, Efflux Pump Inhibiting, and ADMET Properties of Newly Synthesized 1,3,4-Thiadiazole Derivatives**. ChemistrySelect 2021;6:12571–81. https://doi.org/10.1002/slct.202103214.
25. Cos P, Vlietinck AJ, Berghe D Vanden, Maes L. Anti-infective potential of natural products: How to develop a stronger in vitro "proof-of-concept." Journal of Ethnopharmacology 2006;106:290–302. https://doi.org/10.1016/j.jep.2006.04.003.
26. Altuner EM, Canli K, Akata I. Antimicrobial screening of Calliergonella cuspidata, Dicranum polysetum and Hypnum cupressiforme. Journal of Pure and Applied Microbiology 2014;8:539–45.
27. ALTUNER EM, ÇETER T, GÜR M, GÜNEY K, KIRAN B, AKWIETEN HE, et al. Chemical Composition and Antimicrobial Activities of Cold-Pressed Oils Obtained From Nettle, Radish and Pomegranate Seeds. Kastamonu Üniversitesi Orman Fakültesi Dergisi 2018;18:236–47. https://doi.org/10.17475/kastorman.498413.
28. Canli K, Yetgin A, Benek A, Bozyel ME, Altuner EM. In Vitro Antimicrobial Activity Screening of Ethanol Extract of Lavandula stoechas and Investigation of Its Biochemical Composition. Advances in Pharmacological Sciences 2019;2019. https://doi.org/10.1155/2019/3201458.

29. Karaca B, Çöleri Cihan A, Akata I, Altuner EM. Anti-Biofilm and Antimicrobial Activities of Five Edible and Medicinal Macrofungi Samples on Some Biofilm Producing Multi Drug Resistant Enterococcus Strains. Turkish Journal of Agriculture - Food Science and Technology 2020;8:69. https://doi.org/10.24925/turjaf.v8i1.69-80.2723.
30. Xu Z, Liang Y, Lin S, Chen D, Li B, Li L, et al. Crystal Violet and XTT Assays on Staphylococcus aureus Biofilm Quantification. Current Microbiology 2016;73:474–82. https://doi.org/10.1007/s00284-016-1081-1.
31. Vestby LK, Møretrø T, Langsrud S, Heir E, Nesse LL. Biofilm forming abilities of Salmonella are correlated with persistence in fish meal- and feed factories. BMC Veterinary Research 2009;5:1–6. https://doi.org/10.1186/1746-6148-5-20.
32. Martins M, Couto I, Viveiros M, Amaral L. in Bacterial Clinical Isolates by Two Simple Methods. Methods 2010;642:143–57. https://doi.org/10.1007/978-1-60327-279-7.
33. Altınöz E, Altuner EM. Responses of some Escherichia coli clinical isolate strains with multiple drug resistance and overexpressed efux pumps against efux pump inhibitors. International Journal of Biology and Chemistry 2020;13:77–87. https://doi.org/10.26577/ijbch.2020.v13.i1.08.
34. Drug Likeness Tool 2018. http://www.niper.gov.in/pi_dev_tools/DruLiToWeb/DruLiTo_index.html.
35. Daina A, Michielin O, Zoete V. SwissADME: A free web tool to evaluate pharmacokinetics, drug-likeness and medicinal chemistry friendliness of small molecules. Scientific Reports 2017;7:1–13. https://doi.org/10.1038/srep42717.
36. Lipinski CA, Lombardo F, Dominy BW, Feeney PJ. Experimental and computational approaches to estimate solubility and permeability in drug discovery and development settings. Advanced Drug Delivery Reviews 2012;64:4–17. https://doi.org/10.1016/j.addr.2012.09.019.
37. Ghose AK, Viswanadhan VN, Wendoloski JJ. A knowledge-based approach in designing combinatorial or medicinal chemistry libraries for drug discovery. 1. A qualitative and quantitative characterization of known drug databases. Journal of Combinatorial Chemistry 1999;1:55–68. https://doi.org/10.1021/cc9800071.
38. Veber DF, Johnson SR, Cheng HY, Smith BR, Ward KW, Kopple KD. Molecular properties that influence the oral bioavailability of drug candidates. Journal of Medicinal Chemistry 2002;45:2615–23. https://doi.org/10.1021/jm020017n.
39. Egan WJ, Merz KM, Baldwin JJ. Prediction of drug absorption using multivariate statistics. Journal of Medicinal Chemistry 2000;43:3867–77. https://doi.org/10.1021/jm000292e.
40. Muegge I, Heald SL, Brittelli D. Simple selection criteria for drug-like chemical matter. Journal of Medicinal Chemistry 2001;44:1841–6. https://doi.org/10.1021/jm015507e.
41. Dong J, Wang NN, Yao ZJ, Zhang L, Cheng Y, Ouyang D, et al. Admetlab: A platform for systematic ADMET evaluation based on a comprehensively collected ADMET database. Journal of Cheminformatics 2018;10:1–11. https://doi.org/10.1186/s13321-018-0283-x.
42. Cheng F, Li W, Zhou Y, Shen J, Wu Z, Liu G, et al. AdmetSAR: A comprehensive source and free tool for assessment of chemical ADMET properties. Journal of Chemical Information and Modeling 2012;52:3099–105. https://doi.org/10.1021/ci300367a.
43. Yang H, Lou C, Sun L, Li J, Cai Y, Wang Z, et al. AdmetSAR 2.0: Web-service for prediction and optimization of chemical ADMET properties. Bioinformatics 2019;35:1067–9. https://doi.org/10.1093/bioinformatics/bty707.
44. Lee SK, Chang GS, Lee IH, Chung JE, Sung KY NK. The PreADME: Pc-Based program for batch prediction of ADME properties. EuroQSAR 2004;9:5–10.
45. Lee S, Lee IH, Kim H joong, Chang GS, Chung JE, No KT. The PreADME Approach: Web-based program for rapid prediction of physico-chemical, drug absorption and drug-like properties. Euro QSAR 2002 - Designing Drugs and Crop Protectants: Processes Problems and Solutions 2002:418–20.
46. Datar PA. 2D-QSAR Study of Indolylpyrimidines Derivative as Antibacterial against Pseudomonas aeruginosa and Staphylococcus aureus : A Comparative Approach . Journal of Computational Medicine 2014;2014:1–9. https://doi.org/10.1155/2014/765457.
47. Core R Team. A language and environment for statistical computing. Https://WwwR-ProjectOrg/ 2016. https://www.r-project.org/.
48. Şener İ, Şahin Ç, Demir S, Şener N, Gür M. A combined experimental and computational study of electrochemical and photophysical properties of new benzophenone derivatives functionalized with N-substituted-phenyl-1,3,4-thiadiazole-2-amine. Journal of Molecular Structure 2020;1203. https://doi.org/10.1016/j.molstruc.2019.127475.
49. Şener N, Gür M, Çavuş MS, Zurnaci M, Şener İ. Synthesis, Characterization, and Theoretical Calculation of New Azo Dyes Derived from [1,5- a]Pyrimidine-5-one Having Solvatochromic Properties. Journal of Heterocyclic Chemistry 2019;56:1101–10. https://doi.org/10.1002/jhet.3497.
50. Langdon-Jones EE, Hallett AJ, Routledge JD, Crole DA, Ward BD, Platts JA, et al. Using Substituted Cyclometalated Quinoxaline Ligands To Finely Tune the Luminescence Properties of Iridium(III) Complexes. Inorganic Chemistry 2013;52:448–56. https://doi.org/10.1021/ic301853t.
51. Jabłońska-Wawrzycka A, Rogala P, Czerwonka G, Michałkiewicz S, Hodorowicz M, Kowalczyk P. Ruthenium(IV) Complexes as Potential Inhibitors of Bacterial Biofilm Formation. Molecules 2020;25:4938. https://doi.org/10.3390/molecules25214938.
52. Sultana ST, Babauta JT, Beyenal H. Electrochemical biofilm control: a review. Biofouling 2015;31:745–58. https://doi.org/10.1080/08927014.2015.1105222.
53. Samsonoff N. Photosynthetic-Plasmonic-Voltaics: Plasmonically Excited Biofilms for Electricity Production. Master of Applied Science Graduate Department of Mechanical and Industrial Engineering, 2013, p. 100.
54. Nie L, Li Y, Chen S, Li K, Huang Y, Zhu Y, et al. Biofilm Nanofiber-Coated Separators for Dendrite-Free Lithium Metal Anode and Ultrahigh-Rate Lithium Batteries. ACS Applied Materials and Interfaces 2019;11:32373–80. https://doi.org/10.1021/acsami.9b08656.
55. Önkol T, Dogruer D, Uzun L, Adak S, Özkan S, Sahin MF. Synthesis and antimicrobial activity of new 1,2,4-triazole and 1,3,4-thiadiazole derivatives. Journal of Enzyme Inhibition and Medicinal Chemistry 2008;23:277–84. https://doi.org/10.1080/14756360701408697.
56. Otilia Pintilie, Lenuta Profire, Valeriu Sunel MP and AP. Synthesis and Antimicrobial Activity of Some New 1,3,4-Thiadiazole and 1,2,4-Triazole Compounds Having a D,L-Methionine Moiety. Molecules 2007;12:103–13. https://doi.org/10.1007/BF03038821.
57. Zamani, K.; Faghifi, K.; Tefighi, I.; Sharlatzadeh MR. Synthesis and Antimicrobial Activity of Some Pyridyl and Naphthyl Substituted 1 , 2 , 4-Triazole and. Turkish Journal of Chemistry 2004;28:95–100.
58. Richet H, Fournier PE. Nosocomial Infections Caused by Acinetobacter baumannii A Major Threat Worldwide . Infection Control & Hospital Epidemiology 2006;27:645–6. https://doi.org/10.1086/505900.
59. J. Rodrı´guez-Ban˜o, S. Martı´, S. Soto, F. Ferna´ndez-Cuenca, J. M. Cisneros4, J. Pacho´n, A. Pascual, L. Martı´nez- Martı´nez5,

C. McQueary6, L. A. Actis JV and the SG for the S of. Biofilm formation in Acinetobacter baumannii: associated features and clinical implications. Clinical Microbiology and Infection 2008;14:276–8.

60. Jesús Rodríguez-Baño, MD, PhD; Jose M. Cisneros, MD, PhD; Felipe Fernández-Cuenca, MD, PhD; Anna Ribera, MD; Jordi Vila, MD, PhD; Alvaro Pascual, MD, PhD; Luis Martínez-Martínez, MD, PhD; Germán Bou, MD, PhD; Jerónimo Pachón, MD P the G de E de IH (GEIH). Clinical features and epidemiology of Acinetobacter baumanni colonization and infection in Spanish hospitals 2004;25:819–24.
61. Rodríguez-Baño J, Pascual Á, Gálvez J, Muniain MÁ, Ríos MJ, Martínez-Martínez L, et al. Bacteriemias por Acinetobacter baumannii: Características clínicas y pronósticas. Enfermedades Infecciosas y Microbiologia Clinica 2003;21:242–7. https://doi.org/10.1157/13046543.
62. Hatt JK, Rather PN. Role of bacterial biofilms in urinary tract infections. Current Topics in Microbiology and Immunology 2008;322:163–92. https://doi.org/10.1007/978-3-540-75418-3_8.
63. López D, Vlamakis H, Kolter R. Biofilms. Cold Spring Harbor Perspectives in Biology 2010;2. https://doi.org/10.1101/cshperspect.a000398.
64. Jabra-Rizk MA, Falkler WA, Meiller TF. Fungal Biofilms and Drug Resistance. Emerging Infectious Diseases 2004;10:14–9. https://doi.org/10.3201/eid1001.030119.
65. Cascioferro S, Parrino B, Petri GL, Cusimano MG, Schillaci D, Di Sarno V, et al. 2,6-Disubstituted imidazo[2,1-b][1,3,4]thiadiazole derivatives as potent staphylococcal biofilm inhibitors. European Journal of Medicinal Chemistry 2019;167:200–10. https://doi.org/10.1016/j.ejmech.2019.02.007.
66. Minvielle MJ, Bunders CA, Melander C. Indole-triazole conjugates are selective inhibitors and inducers of bacterial biofilms. MedChemComm 2013;4:916–9. https://doi.org/10.1039/c3md00064h.
67. Markou G, Georgakakis D. Cultivation of filamentous cyanobacteria (blue-green algae) in agro-industrial wastes and wastewaters: A review. Applied Energy 2011;88:3389–401. https://doi.org/10.1016/j.apenergy.2010.12.042.
68. Rahman A, Agrawal S, Nawaz T, Pan S, Selvaratnam T. A review of algae-based produced water treatment for biomass and biofuel production. Water (Switzerland) 2020;12:1–27. https://doi.org/10.3390/W12092351.
69. Webber MA, Piddock LJV. The importance of efflux pumps in bacterial antibiotic resistance. Journal of Antimicrobial Chemotherapy 2003;51:9–11. https://doi.org/10.1093/jac/dkg050.
70. Pogrebnoi S, Chiriţă C, Valica V, Macaev F, Chifiriuc MC, Kamerzan C, et al. Studies on the antimycobacterial action of a novel compound of the thiadiazole class, 2-(Propyl-thio)-5H-[1,3,4]-thiadiazole[2,3-B]-quinazoline-5-one. Farmacia 2017;65:69–74.
71. Zeng B, Wang H, Zou L, Zhang A, Yang X, Guan Z. Evaluation and target validation of indole derivatives as inhibitors of the AcrAB-TolC efflux pump. Bioscience, Biotechnology and Biochemistry 2010;74:2237–41. https://doi.org/10.1271/bbb.100433.
72. Nikaido E, Shirosaka I, Yamaguchi A, Nishino K. Regulation of the AcrAB multidrug efflux pump in Salmonella enterica serovar Typhimurium in response to indole and paraquat. Microbiology 2011;157:648–55. https://doi.org/10.1099/mic.0.045757-0.
73. Molina-Santiago C, Daddaoua A, Fillet S, Duque E, Ramos JL. Interspecies signalling: Pseudomonas putida efflux pump TtgGHI is activated by indole to increase antibiotic resistance. Environmental Microbiology 2014;16:1267–81. https://doi.org/10.1111/1462-2920.12368.
74. Artursson P. Epithelial transport of drugs in cell culture. I: A model for studying the passive diffusion of drugs over intestinal absorbtive (Caco-2) cells. Journal of Pharmaceutical Sciences 1990;79:476–82. https://doi.org/10.1002/jps.2600790604.
75. Kratochwil NA, Huber W, Müller F, Kansy M, Gerber PR. Predicting plasma protein binding of drugs: A new approach. Biochemical Pharmacology 2002;64:1355–74. https://doi.org/10.1016/S0006-2952(02)01074-2.
76. Palleria C, Di Paolo A, Giofrè C, Caglioti C, Leuzzi G, Siniscalchi A, et al. Pharmacokinetic drug-drug interaction and their implication in clinical management. Journal of Research in Medical Sciences : The Official Journal of Isfahan University of Medical Sciences 2013;18:601–10.
77. Sonkusre P. Specificity of Biogenic Selenium Nanoparticles for Prostate Cancer Therapy With Reduced Risk of Toxicity: An in vitro and in vivo Study. Frontiers in Oncology 2020;9:1–11. https://doi.org/10.3389/fonc.2019.01541.
78. Fromm MF. Importance of P-glycoprotein at blood-tissue barriers. Trends in Pharmacological Sciences 2004;25:423–9. https://doi.org/10.1016/j.tips.2004.06.002.
79. Elmeliegy M, Vourvahis M, Guo C, Wang DD. Effect of P-glycoprotein (P-gp) Inducers on Exposure of P-gp Substrates: Review of Clinical Drug–Drug Interaction Studies. Clinical Pharmacokinetics 2020;59:699–714. https://doi.org/10.1007/s40262-020-00867-1.
80. Pardridge WM. Blood-brain barrier delivery. Drug Discovery Today 2007;12:54–61. https://doi.org/10.1016/j.drudis.2006.10.013.
81. Fong CW. Permeability of the Blood–Brain Barrier: Molecular Mechanism of Transport of Drugs and Physiologically Important Compounds. Journal of Membrane Biology 2015;248:651–69. https://doi.org/10.1007/s00232-015-9778-9.
82. Nielsen PA, Andersson O, Hansen SH, Simonsen KB, Andersson G. Models for predicting blood-brain barrier permeation. Drug Discovery Today 2011;16:472–5. https://doi.org/10.1016/j.drudis.2011.04.004.
83. Muehlbacher M, Spitzer GM, Liedl KR, Kornhuber J. Qualitative prediction of blood-brain barrier permeability on a large and refined dataset. Journal of Computer-Aided Molecular Design 2011;25:1095–106. https://doi.org/10.1007/s10822-011-9478-1.
84. Wilkinson GR, Shand DG. A physiological approach to hepatic drug clearance. Clinical Pharmacology & Therapeutics 1975;18:377–90. https://doi.org/10.1002/cpt1975184377.
85. Ye M, Nagar S, Korzekwa K. A physiologically based pharmacokinetic model to predict the pharmacokinetics of highly protein-bound drugs and the impact of errors in plasma protein binding. Biopharmaceutics & Drug Disposition 2016;37:123–41. https://doi.org/10.1002/bdd.1996.
86. Guengerich,Peter F. Cytochromes P450, Drugs, and Diseases. Molecular Interventions 2003;3:194–204.
87. Zanger UM, Schwab M. Cytochrome P450 enzymes in drug metabolism: Regulation of gene expression, enzyme activities, and impact of genetic variation. Pharmacology and Therapeutics 2013;138:103–41. https://doi.org/10.1016/j.pharmthera.2012.12.007.
88. Kerns EH, Di L. Drug-like Properties: Concepts, Structure Design and Methods. Drug-like Properties: Concepts, Structure Design and Methods 2008.
89. Xu Y, Dai Z, Chen F, Gao S, Pei J, Lai L. Deep Learning for Drug-Induced Liver Injury. Journal of Chemical Information and Modeling 2015;55:2085–93. https://doi.org/10.1021/acs.jcim.5b00238.
90. Wang S, Li Y, Wang J, Chen L, Zhang L, Yu H, et al. ADMET evaluation in drug discovery. 12. Development of binary

classification models for prediction of hERG potassium channel blockage. Molecular Pharmaceutics 2012;9:996–1010. https://doi.org/10.1021/mp300023x.

91. Zeiger E. The test that changed the world: The Ames test and the regulation of chemicals. Mutation Research - Genetic Toxicology and Environmental Mutagenesis 2019;841:43–8. https://doi.org/10.1016/j.mrgentox.2019.05.007.

92. Fujita Y, Honda H, Yamane M, Morita T, Matsuda T, Morita O. A decision tree-based integrated testing strategy for tailor-made carcinogenicity evaluation of test substances using genotoxicity test results and chemical spaces. Mutagenesis 2019;34:3–16. https://doi.org/10.1093/mutage/gey039.

APPENDIX

S1. Experimental results for all synthesized compounds are presented in Table 1.

Table 1. Experimental data of all synthesized compounds

Compounds	Molecular formula	Molecular weight	Yield (%)	Melting point	Colour
C1	$C_{29}H_{32}N_6OS_2$	544.73	-	175°C	Yellow
C2	$C_{30}H_{21}N_6OS_2$	545.65	-	186°C	Dark brown
C3	$C_{211}H_{20}N_6OS_2$	436.55	-	225°C	Light brown
C4	$C_{33}H_{28}N_6OS_2$	588.74	-	270°C	Ligt yellow

S2. FT-IR spectrum of all compounds are given in Figure 1-4.

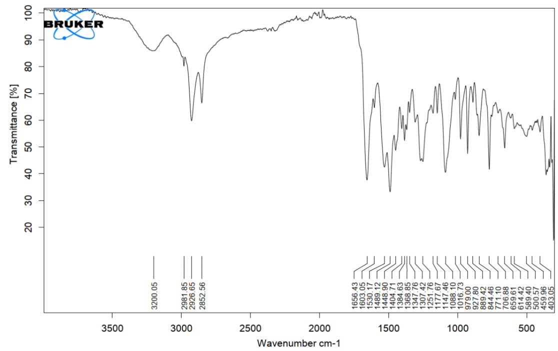

Figure 1. FT-IR spectrum of compound C1.

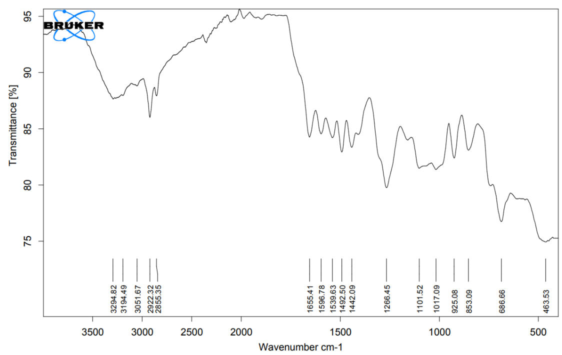

Figure 2. FT-IR spectrum of compound C2

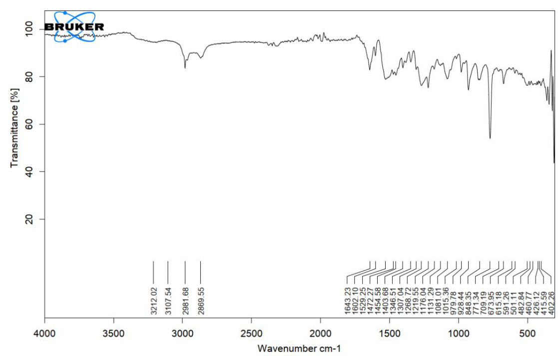

Figure 3. FT-IR spectrum of compound C3

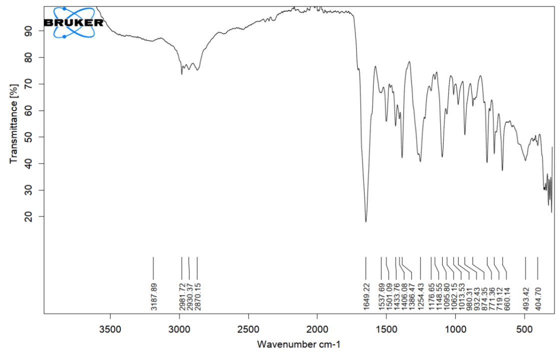

Figure 4. FT-IR spectrum of compound C4

S3. [13]C-NMR spectrum of all compounds are given in Figure 5-7.

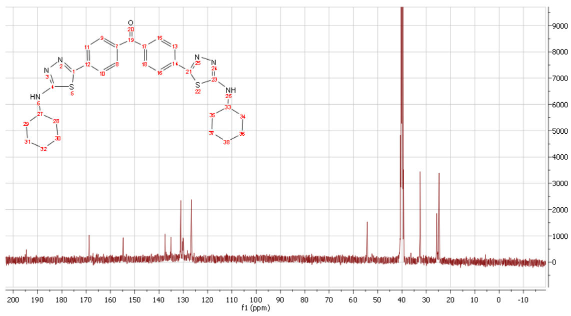

Figure 5. ^{13}C-NMR spectrum of compound C1

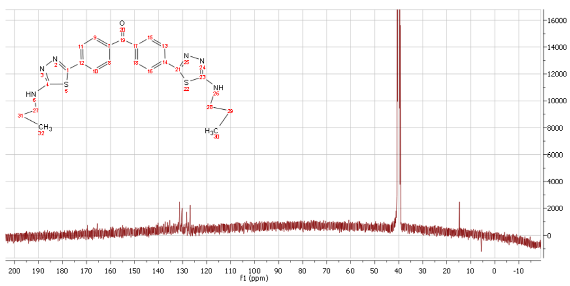

Figure 6. ^{13}C-NMR spectrum of compound C3

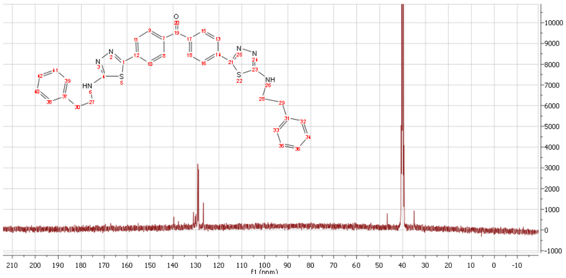

Figure 7. ^{13}C-NMR spectrum of compound C4

S4. ^{1}H-NMR spectrum of all compounds are given in Figure 8-11.

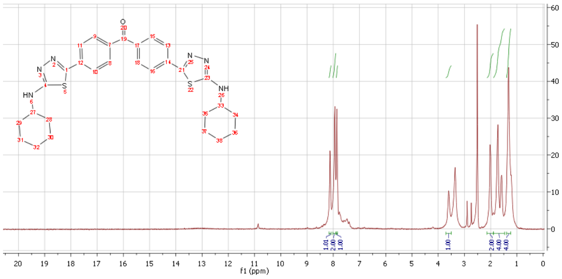

Figure 8. ^{1}H-NMR spectrum of compound C1

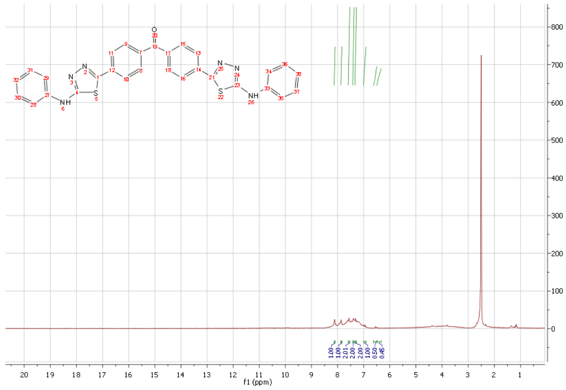

Figure 9. ^{1}H-NMR spectrum of compound C2

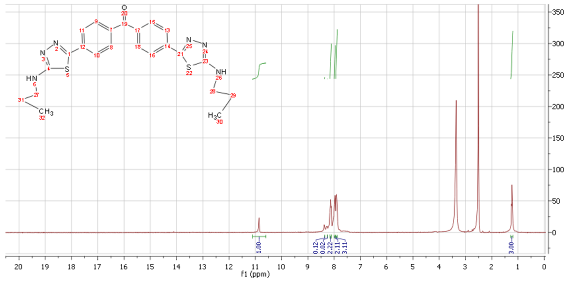

Figure 10. ^{1}H-NMR spectrum of compound C3

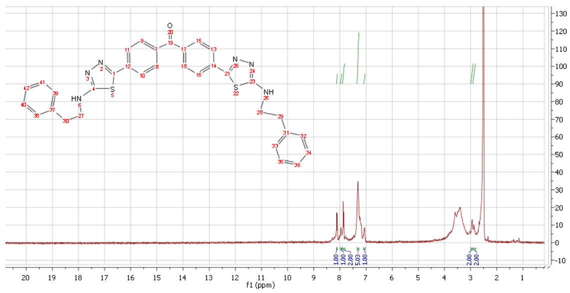

Figure 11. ^{1}H-NMR spectrum of compound C4